Bloch oscillations of magnetic solitons in anisotropic spin-$\frac{1}{2}$ chains

Jordan Kyriakidis* and Daniel Loss†
Department of Physics and Astronomy, University of Basel, Klingelbergstrasse 82, CH-4056 Basel, Switzerland
(Received 12 March 1998)

We study the quantum dynamics of solitonlike domain walls in anisotropic spin-$\frac{1}{2}$ chains in the presence of magnetic fields. In the absence of fields, domain walls form a Bloch band of delocalized quantum states while a static field applied along the easy axis localizes them into Wannier wave packets and causes them to execute Bloch oscillations, i.e., the domain walls oscillate along the chain with a finite Bloch frequency and amplitude. In the presence of the field, the Bloch band, with a continuum of extended states, breaks up into the Wannier-Zeeman ladder—a discrete set of equally spaced energy levels. We calculate the dynamical structure factor $S^{zz}(q,\omega)$ in the one-soliton sector at finite frequency, wave vector, and temperature, and find sharp peaks at frequencies which are integer multiples of the Bloch frequency. We further calculate the uniform magnetic susceptibility and find that it too exhibits peaks at the Bloch frequency. We identify several candidate materials where these Bloch oscillations should be observable, for example, via neutron-scattering measurements. For the particular compound $CoCl_2 \cdot 2H_2O$ we estimate the Bloch amplitude to be on the order of a few lattice constants, and the Bloch frequency on the order of 100 GHz for magnetic fields in the Tesla range and at temperatures of about 18 K. [S0163-1829(98)06933-1]

I. INTRODUCTION

Bloch oscillations[1–3] of a quantum state in a periodic one-dimensional structure can be characterized as an *oscillatory* response to a *constant* force. The phenomenon is a remarkable example of the counterintuitive nature of quantum mechanics. Not only does the particle oscillate in response to a static and homogeneous force, but the amplitude of the oscillation is *inversely* proportional to the magnitude of the force.

The prototypical system in which to observe Bloch oscillations (BO's) has historically been a band electron in an external electric field.[1–3] In the absence of inelastic scattering and interband (Zener) transitions, the electron, in momentum space, continually traverses the Brillouin zone. Upon reaching a zone boundary, the electron is reflected to the opposite boundary and thereby reverses its momentum. In real space, the motion is likewise periodic—a constant force thus produces oscillatory motion. But the existence of BO's has been controversial ever since its theoretical prediction many decades ago (Ref. 2 contains an early review). The controversy surrounding the theory was largely concerned with the use, or rather the misuse, of Bloch's theorem in systems where the lattice periodicity was explicitly broken by a constant external field. Experiments were not conclusive because, in these early times, bulk solids were the only systems available. Their bandwidths, however, are typically too large, the lattice constants too small, and the inelastic scattering so frequent that the phase coherence of the particle state, essential for the existence of BO's, is rapidly destroyed.

However, with the advent of semiconductor heterostructures—in particular layered superlattices with large lattice constants, and thus small bandwidths, which allow many coherent BO's before phase coherence is lost—the debate about BO's seems to be settled. Recent experiments now provide convincing evidence that BO's of electrons can indeed occur. This confirmation comes from the detection of the coherent radiation emitted as ensembles of electrons execute BO's.[4] There is also work which directly measures the physical displacement of electrons in superlattices as they oscillate.[5]

The search for BO's has not been limited to electrons. Recently, the effect was observed with ultracold atoms placed in an optical standing wave.[6] The standing wave served as the periodic potential, and a force was simulated by accelerating this periodic potential. The momentum distribution of the atoms had the time dependence expected from the theory of BO's.

Current studies of BO's are moving beyond the establishment of their existence. In atom-optical systems, BO's are being used to test other aspects of quantum theory. For example, nonexponential decay of unstable systems was very recently observed in the same systems used to observe BO's and the Wannier-Stark ladder.[7] In electronic systems, BO's are being studied as a means of producing fast emitters of coherent radiation. The radiation emitted by the oscillating charges can be tuned over a wide range of frequencies simply by changing the electric-field strength. Typical wavelengths are in the submillimeter range.

An entirely different class of systems in which such coherence phenomena can be expected are magnetic systems, which brings us to the main subject of this work. It has been pointed out recently that BO's should exist in purely magnetic systems—in the quantum dynamics of domain walls with solitonlike behavior.[8] This proposal for magnetic BO's was based on a semiclassical treatment[9] of the quantum dynamics of extended domain walls moving in a periodic potential and containing a large number of spins s, with $s \gg 1$. In the present work, we shall extend this investigation to the fully quantum-mechanical regime of anisotropic spin-$\frac{1}{2}$ chains and demonstrate that BO's occur in the quantum dynamics of elementary excitations such as spin solitons. Such solitons represent the extreme limit of a magnetic domain

wall with a width of only one lattice constant. In contrast to the cases mentioned above (electrons and atoms), magnetic BO's are an inherently many-body effect. The soliton motion is a cooperative phenomenon resulting from spin-spin interaction. Nevertheless, we will see that magnetic BO's share many properties with their electronic counterpart.

A remarkable feature of magnetic BO's is that they give rise to oscillations of the magnetization at a Bloch frequency which can be continuously varied by an external magnetic field. Thus, besides being of fundamental interest, BO's of magnetic solitons may also prove relevant for applications since they provide a natural source of *magnetic* dipole radiation—typically in the microwave regime.

The outline of this work is as follows. In the next section, we define and discuss the one-soliton approximation in the presence of a magnetic field B applied along the easy axis, thereby extending the zero-field results obtained previously for antiferromagnets[10] (AFM's) and for ferromagnets (FM's).[11] We show that the external B field localizes the eigenstates of the Bloch band and discretizes the spectrum into a set of equally spaced levels which we call the Wannier-Zeeman ladder (WZL), in analogy to the Wannier-Stark ladder in electronic systems. We mention several spin models capable of supporting BO's, but our main focus is on Ising-like FM chains with biaxial anisotropy—a model which accurately describes compounds such as[12] $CoCl_2 \cdot 2H_2O$. We then go on to discuss the spin correlation functions and calculate the wave vector and frequency-dependent dynamical structure factor $S^{zz}(q,\omega)$ for two cases: zero and finite magnetic fields. For finite magnetic fields, the structure factor consists of peaks at frequencies corresponding to integer multiples of the Bloch frequency. These frequencies are typically in the GHz range. This result means that, for example, neutron-scattering measurements on samples in thermal equilibrium can be used to observe the WZL. In zero magnetic field, we obtain a structure factor for FM's that is very similar in form to the one obtained for AFM's,[10] apart from a wave-vector dependence that reflects the difference in magnetic ordering between FM's and AFM's. After a brief digression on the $B \to 0$ limit, we turn to an investigation of specific materials which are promising candidates in which to observe BO of magnetic solitons. We focus on one particular Ising-like FM,[12] $CoCl_2 \cdot 2H_2O$, which appears to be the best characterized of the ones we have identified. Other materials, though less well characterized, are potentially better candidates. Finally, we close with a summary of the main results, along with an outlook on future directions.

II. THE ONE-SOLITON APPROXIMATION

In the following we concentrate on one-dimensional Ising-like magnets with nearest-neighbor exchange interactions J^α and in the presence of a magnetic field $\mathbf{b}_n = g\mu_B \mathbf{B}_n$. The general anisotropic spin Hamiltonian is given by

$$H = -\sum_{n,\alpha} (J^\alpha S_n^\alpha S_{n+1}^\alpha + b_n^\alpha S_n^\alpha), \tag{1}$$

where n denotes lattice sites and α denotes Cartesian coordinates. The exchange constants J^α are either positive (FM's) or negative (AFM's), with $|J^z| \gg |J^{x,y}|$. Thus, the (Ising) easy axis is along the z axis. In systems with such a strong easy axis, domain walls, or solitons (we shall use these terms interchangeably), are well defined. At sufficiently low temperatures, the system is in its ground state: ferromagnetic order for FM's, and Néel order for AFM's. The excitations consist of domain walls. In a pure Ising chain ($J^x = J^y = 0$) with zero field ($b_n^\alpha = 0$), the spectrum consists of discrete energy levels, where each level corresponds to states with a fixed number of domain walls. If, as is usually the case, there are additional exchange couplings in the directions transverse to the Ising axis ($J^x \neq 0$ or $J^y \neq 0$), then the degeneracy is lifted. The energy spectrum consists of a series of continua separated by gaps. Each continuum consists of states with a fixed number of domain walls. The one-soliton approximation considers only the lowest band and neglects all transitions to higher bands.

The spectrum described in the preceding paragraph has been verified numerically[13] for the anisotropic x-y model; for very large anisotropy (near the Ising limit), isolated bands with large gaps were observed, with the gap tending to zero as the isotropic limit was approached. The one-soliton approximation was used by Villain[10] in his pioneering work on spin-$\frac{1}{2}$ solitons in Ising-like AFM chains. The result of his calculation—the existence of a dispersive soliton mode (the Villain mode) below the two-particle continuum—was further verified by theoretical[14] and numerical[15] work, inelastic neutron-scattering experiments on the Ising-like AFM's $CsCoCl_3$ (Refs. 16,17) and $CsCoBr_3$ (Refs. 18,19), as well as electron-spin resonance,[20] nuclear magnetic resonance,[21] and optical[22] experiments.

Analytic work guided by physical reasoning, exact numerical work on finite systems, and experimental work on real physical systems all point to the existence of the Villain mode and thus justify the one-soliton approximation. What then are the conditions necessary for the Villain mode to exist? Two conditions should be met. First, a large easy axis is required; the system must be near the Ising limit. This ensures not only that domain walls are well-defined excitations, but also that states with different numbers of domain walls are well separated in energy. Second, the domain walls must have dynamics. It is the dynamics of the domain walls which induce the band structure. In a pure Ising chain, for example, a localized domain wall is an eigenstate of the Hamiltonian and therefore has no dynamics. The Villain mode does not exist in pure Ising chains.

Most of the existing work has focused so far on AFM's, and only recently has it been pointed out that dispersive soliton modes can also exist in Ising-like FM's (Ref. 11) and other spin chains, as discussed next.

A. Primary model

In view of the candidate materials to be identified in Sec. IV, we focus mainly on spin-$\frac{1}{2}$ FM's with a Hamiltonian given by Eq. (1) with $J^\alpha > 0$.[11] We consider a static and homogeneous field b along the z axis (the Ising direction) and rewrite the Hamiltonian in a more suggestive form:

$$H = H^I + H^a + H^\perp, \tag{2a}$$

$$H^I = -J^z \sum_n S_n^z S_{n+1}^z - b \sum_n S_n^z, \tag{2b}$$

$$H^a = -\frac{1}{4}(J^x - J^y) \sum_n (S_n^+ S_{n+1}^+ + S_n^- S_{n+1}^-), \tag{2c}$$

$$H^\perp = -\frac{1}{4}(J^x + J^y) \sum_n (S_n^+ S_{n+1}^- + S_n^- S_{n+1}^+), \tag{2d}$$

where $S_n^\pm = S_n^x \pm i S_n^y$ are the usual raising and lowering operators. In preparation for the one-soliton approximation, we introduce the one-soliton states $\{|m,Q\rangle\}$, defined by

$$|m,1\rangle = |\cdots \overset{m}{\uparrow\uparrow}\downarrow\downarrow\cdots\rangle, \quad |m,-1\rangle = |\cdots \overset{m}{\downarrow\downarrow}\uparrow\uparrow\cdots\rangle. \tag{3}$$

The right-hand sides are expressed in the S^z basis. Here, $m = 0, \pm 1, \pm 2, \ldots$ denotes the soliton position ($m=0$ corresponds to the center of the spin chain), and $Q = \pm 1$ is the charge of the soliton. We can define the soliton position, charge, and translation operators—$\hat{m}$, $\hat{Q}$, and $\hat{T}_n$, respectively—as

$$\hat{m}|m,Q\rangle = m|m,Q\rangle,$$

$$\hat{Q}|m,Q\rangle = Q|m,Q\rangle, \tag{4}$$

$$\hat{T}_n|m,Q\rangle = |m+n,Q\rangle,$$

where $\hat{m}$ and $\hat{Q}$ are Hermitian operators, whereas $\hat{T}_n$ is unitary with $\hat{T}_n^\dagger = \hat{T}_{-n}$.

The one-soliton approximation is tantamount to considering our system as containing one domain wall and discarding those terms in Eq. (2) which create additional solitons. For example, $H^\perp$ in Eq. (2d) should be discarded because these terms will always create solitons, but H^a in Eq. (2c) contains terms which translate the soliton by two sites, which will be identified with $\hat{T}_2$ and $\hat{T}_2^\dagger$. Projecting Eq. (2) onto the one-soliton subspace, we therefore obtain

$$H_{1\text{-sol}} = \frac{1}{2}J^z + \Delta(T_2 + T_{-2}) - bQm,$$

$$\Delta = (J^y - J^x)/4, \tag{5}$$

where we have dropped the hats over the operators, and are measuring energy relative to the fully polarized (ferromagnetic) state. The bandwidth Δ is different from zero only if $J_x \neq J_y$, in contrast to AFM's or alternate field configurations (see below). In what follows, we shall work in a fixed charge sector. Thus, Q is effectively a constant and we will set $Q = -1$ to be definite. Equation (5) is then formally equivalent to a single-band tight-binding model of an electron in an external electric field. Solitons play the role of electrons, and a magnetic field the role of the electric field. We can now go on to discuss the eigenstates and energy spectrum, both of which are qualitatively very different in the finite- and zero-field regimes, respectively. Bloch oscillations can be derived either semiclassically from the zero-field solution, or fully quantum mechanically from the finite-field solutions. We discuss each of these in turn.

1. Semiclassical solution

We will first consider the known physics in zero external field in order to make contact with previous work on AFM's,[10] FM's,[11] as well as with semiclassical derivations of BO's. For $b=0$, and with periodic boundary conditions, the eigenstates of Eq. (5) describing the soliton are extended Bloch states labeled by the wave vector k:

$$|k,Q\rangle = \frac{1}{\sqrt{N_{\text{tot}}}} \sum_m e^{ikm}|m,Q\rangle. \tag{6}$$

Here, we have set the lattice constant a equal to one. The periodic dispersion relation resulting from these eigenstates is given by[11]

$$E(k) = \frac{1}{2}J^z + 2\Delta \cos(2k). \tag{7}$$

This is the ferromagnetic analog of Villain's result[10] for AFM's. As mentioned below, Villain's result for the bandwidth Δ contains the sum, rather than the difference, of the transverse couplings.

Semiclassically, we can reproduce the derivation of BO's as it is given in conventional electronic treatments.[3,23] In the absence of scattering, the effect of the field-dependent term bQm in Eq. (5) is to drive the soliton through the band. The velocity $v(k)$ of this motion is found by differentiating Eq. (7) with respect to k. On the other hand, the wave vector k acquires a time dependence through the force $F = \hbar\dot{k} = b/a$. Integrating $v(k(t))$ over time then yields the semiclassical Bloch oscillations. If $x(t)$ denotes the soliton position, then

$$x(t) = \text{const} - \frac{1}{2}A_B \cos(\omega_B t), \tag{8}$$

with the Bloch amplitude A_B and the Bloch angular frequency ω_B given by

$$A_B = 4\Delta a/b, \quad \hbar\omega_B = 2b = 2g\mu_B B. \tag{9}$$

2. Quantum solution (Exact)

We can compare the above semiclassical derivation of BO's with a fully quantum treatment by keeping a nonzero magnetic field in the Hamiltonian right from the outset. For a spin-$\frac{1}{2}$ chain with $N_{\text{tot}} = 2N+1$ sites, and with $b>0$, we can exactly diagonalize Eq. (5) to yield energy eigenstates

$$|E_m\rangle = \sum_{n=-N}^{N} C_{mn}|n\rangle, \tag{10a}$$

$$C_{mn} = \langle n|E_m\rangle = \frac{1+(-1)^{m-n}}{2} J_{(m-n)/2}(\alpha), \quad \alpha = \Delta/b, \tag{10b}$$

where J_n is the ordinary Bessel function of order n, and we have dropped the label $Q=-1$ in the state vectors. The state $|E_m\rangle$ is *localized* about the lattice site m in the sense that $\lim_{n\to\infty}\langle n|E_m\rangle = 0$ for arbitrary m. We have thus chosen vanishing boundary conditions—a reasonable choice for localized states. The degree of localization is given by the argument of the Bessel function [see Eq. (14) below]; strong

fields act to localize the states. For example, if $b\to\infty$, then $\alpha\to 0$, and only the $m=n$ term contributes to the sum in Eq. (10) since $J_n(0)=\delta_{n,0}$. The eigenstate is therefore strongly localized. As the field decreases, the wave packet spreads. The eigenstates at finite b are Wannier-like states and are thus qualitatively different from the extended Bloch states at zero field. This difference is also reflected in the energy spectrum:

$$\begin{aligned} H_{1\text{-sol}}|E_m\rangle &= \sum_n C_{m,n}[\Delta(|n+2\rangle+|n-2\rangle)+bn|n\rangle] \\ &= \sum_n [\Delta(C_{m,n-2}+C_{m,n+2})+bnC_{m,n}]|n\rangle \\ &= \sum_n \left[\Delta\frac{2}{\alpha}\left(\frac{m-n}{2}\right)C_{m,n}+bnC_{m,n}\right]|n\rangle \\ &= bm\sum_n C_{m,n}|n\rangle = bm|E_m\rangle, \end{aligned} \tag{11}$$

and thus

$$E_m = bm. \tag{12}$$

The important first term on the third line in Eq. (11) was obtained using the Bessel function identity[24] $zJ_{\nu-1}(z)+zJ_{\nu+1}(z)=2\nu J_\nu(z)$. The spectrum $\{E_m\}$ is *discrete*. It consists of a series of equally spaced levels with an energy-level spacing given by b. The analog of this spectrum for electronic systems, which has been observed experimentally,[25] is known as the Wannier-Stark ladder. Hence, for magnetic solitons, the term Wannier-*Zeeman* ladder (WZL) seems appropriate and we shall adopt this term below.

The states $\{|E_m\rangle\}$ are exact eigenstates only up to boundary terms:

$$H_{1\text{-sol}}|E_m\rangle = bm|E_m\rangle + \text{boundary terms}, \tag{13a}$$

where a typical boundary term is given by

$$J_{[m\pm(N+2)]/2}(\alpha)|\pm N\rangle. \tag{13b}$$

For large N and finite b (hence finite α), these boundary terms are negligible contributions. The soliton dynamics are not expected to depend on the boundary conditions for sufficiently large chains, especially since the soliton eigenstates $|E_m\rangle$ are strongly localized by the field. For $n\equiv|m-N|/2\gg 1$, and fixed, finite α, the Bessel function in Eq. (13b) can be replaced by its asymptotic form[24]

$$J_n(\alpha)\approx\frac{1}{\sqrt{2\pi n}}\left(\frac{e\alpha}{2n}\right)^n,\quad (n\gg 1), \tag{14}$$

and therefore decays as n^{-n}, *provided* the argument α remains fixed at some finite value. If $N\gg 1$, and assuming α is indeed fixed, then the correction terms in Eq. (13) can be neglected so long as the center of the eigenstate wavepacket is not near the boundaries of the chain. Exact numerical diagonalization of finite chains (see below) indicates that the states $\{|E_m\rangle\}$ can be considered eigenstates everywhere except at a small, b-dependent boundary layer on either end of the chain. The correction terms can hence be considered surface effects which become negligible in the thermodynamic limit.

More severe problems arise in the limit of vanishing field ($\alpha\to\infty$). In this limit, the above asymptotic form of the Bessel functions cannot be used since now *both* the order of the Bessel function ($\propto N$) as well as its argument ($\propto 1/b^z$) diverge. The appropriate asymptotic form for $J_n(\alpha)$ depends on the ratio n/α; for both $\alpha\to\infty$ and $n\to\infty$ (with $n>\alpha\gg 1$), we have[24]

$$J_n(\alpha)\approx\sqrt{\frac{1}{2\pi}}\left(\frac{1}{n^2-\alpha^2}\right)^{1/4}\left(\frac{\alpha}{n+\sqrt{n^2-\alpha^2}}\right)^n e^{\sqrt{n^2-\alpha^2}}. \tag{15}$$

This expression reduces to Eq. (14) in the limit $n\gg\alpha$. Equation (15) shows that $J_n(\alpha)$ is negligible *only if* $|n^2-\alpha^2|\gg 1$. This effectively implies that no matter how large the system size becomes, there will always be a field sufficiently small, such that the present framework fails. In practice, this becomes problematic only when discussing the ''Villain limit'' of vanishing field, where, in any case, soliton collisions must explicitly be considered (see below).

Another approach is to compare the analytic spectrum $E_m=bm$ with that obtained by numerically diagonalizing finite chains (using $H_{1\text{-sol}}$). In Fig. 1(a), we plot the results for $b/\Delta=3$. This shows that for such fields, our analytic expressions are quite good and can be used with confidence. By contrast, Fig. 1(b) shows a comparison of numeric and analytic results for $b/\Delta=5/N$. We see here that the width of the boundary layer has increased greatly. [The boundary layer consists of those points which deviate substantially from the linear analytic result. In Fig. 1(a), the boundary layer is not discernible.] The boundary layer is not a function of N. It is a function of b. As N increases with b fixed, the boundary layer therefore becomes less and less important. Nevertheless, as b tends to zero, the boundary layer increases until eventually the present framework of localized eigenfunctions must be abandoned. This is our first indication of the problems associated with the $b\to 0$ limit. We shall return to this limit below in connection with the calculation of the dynamical structure factor. For most of this paper, however, we shall consider either sufficiently large fields such that Fig. 1(a) is the relevant scenario, or zero fields, where a dispersive mode with Bloch-like extended states is the correct description. These are the two experimentally relevant regions within the one-soliton approximation.

Assuming a sufficiently large field (in the sense of the previous paragraph) and neglecting surface effects, the spectrum of Eq. (5) is the WZL, $E_m=bm$. The presence of the magnetic field thus destroys the continuous band structure of Eq. (7) and replaces it with an evenly spaced ladder of energy levels, with the spacing between adjacent levels given by b. How are BO's manifested within this fully quantum-mechanical framework? To compare with the semiclassical result of Eqs. (8) and (9), we should specify an initial state and compute the expectation value of $\hat{m}$ as a function of time. Let us keep the initial state arbitrary and write $|\psi(0)\rangle=\Sigma_m C_m|E_m\rangle$. Then,

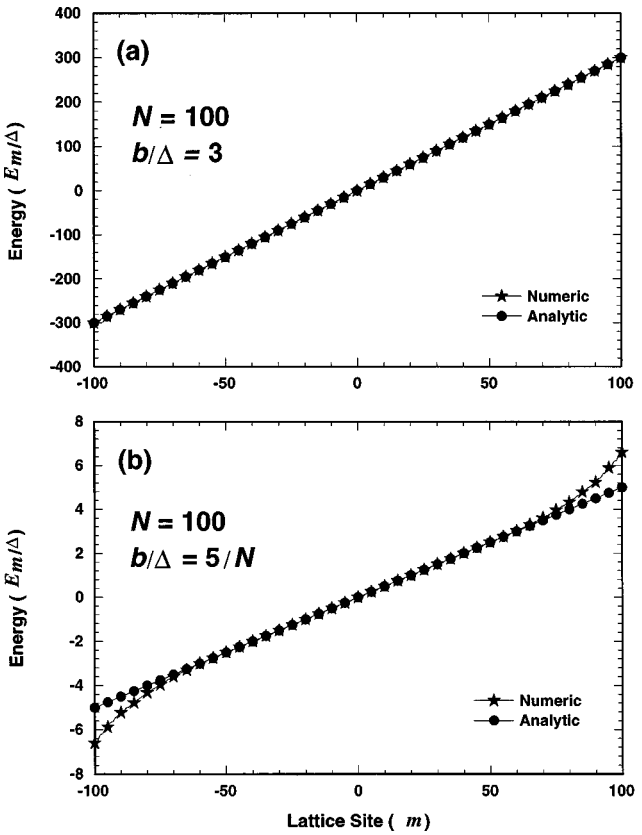

FIG. 1. (a) Comparison of numerical and analytical results for the energy spectrum of Eq. (5) for moderate field values. Only every fifth energy level is shown. (There is one level at each integer value of m.) For such fields, the analytic spectrum $E_m = bm$ is essentially exact. (b) The same plot as in (a), but with a much smaller field. Here, about 20% of the points show significant deviation between the analytic and numerical results. As b continues to decrease, this boundary region increases. For such low fields, the system exhibits approximate translational invariance and so a momentum representation becomes more appropriate.

$$\langle m(t)\rangle = \langle \psi(t)|m|\psi(t)\rangle = \sum_m m|C_m|^2 - \frac{1}{2}A_B \mathrm{Re}\left(e^{-i\omega_B t} \sum_m C_m^* C_{m-2} \right), \tag{16}$$

where Re denotes the real part. If we assume, for example, that all C_m are real, and also that $\Sigma_m C_m C_{m-2} = 1$, then the oscillating piece of Eq. (16) is identical to the oscillating piece of Eq. (8). However, if we take as the initial state one which is completely localized at one lattice site, $|\psi(0)\rangle = |m\rangle$, then the oscillating piece identically vanishes. This situation corresponds to the state vector evolving symmetrically about both sides of the initial position m in a sort of breather state. Thus, the behavior depends sensitively upon the initial conditions.

Semiclassically, we have seen that BO's result from the soliton being pushed unscattered through the band and undergoing Bragg reflection at the zone boundary. By contrast, in a full quantum treatment, BO's result from the time evolution of a state which is not a (Wannier-Zeeman) eigenstate of the Hamiltonian. The frequency of oscillation is given by twice the energy between adjacent states. This is a result of the fact that Eq. (5), with $b = 0$, contains an intrinsic periodicity of *two* lattice constants, which also accounts for the fact that the Brillouin zone is halved, as shown by Eq. (7). This effect can be understood semiclassically in terms of the Berry phase of the spins and is a result of the spin parity (see Ref. 9 for more details).

Finally, we note that BO's are a many-body effect which should be distinguished from Larmor precession of uncoupled spins in an external field. The former yields an oscillating magnetic moment along the direction of the applied field whereas the latter yields oscillations in directions transverse to the field.

We have focused on biaxial FM's because the materials we have identified as candidates for observing BO's are all biaxial FM's. In the next subsection, we show that BO's of magnetic solitons can also exist in uniaxial FM's ($J^x = J^y$) if the field is tilted away from the Ising axis. We also show that BO's exist in anisotropic AFM's if an inhomogeneous field is applied.

B. Other models

1. Ferromagnets

It is not necessary to have a biaxial FM in order to create BO's. In fact, a uniaxial FM ($J^x = J^y$) may be preferable because the bandwidth can then be externally controlled. For example, consider Eq. (1) with ferromagnetic couplings, with $J^x = J^y$, and with a homogeneous magnetic field along both the x and z axes (z is still the Ising axis). The Hamiltonian is almost the same as Eq. (2); the differences are that H^a now vanishes (because $J^x = J^y$) and there is a new term coming from the field in the x direction:

$$H^{a\prime} = -\frac{1}{2} b^x \sum_n (S_n^+ + S_n^-). \tag{17}$$

This term gives hopping by one site. The one-soliton Hamiltonian is

$$H_{1\text{-sol}}^{\text{uni}} = \frac{1}{2}J^z - \frac{1}{2}b^x(T_1 + T_{-1}) - b^z Q m, \tag{18}$$

which is practically identical to Eq. (5). Thus, uniaxial FM's exhibit the WZL if the external field is tilted away from the Ising axis. The important difference between this and the biaxial case is that now the strength of *both* terms are adjustable externally. The energy eigenvalues here are as in Eq. (12), but the eigenstates are replaced by

$$|E_m\rangle^{\text{uni}} = \sum_n J_{m-n}(-b^x/b^z)|n\rangle. \tag{19}$$

Although some of the materials we will identify in the following sections are reported to have only uniaxial anisotropy, the material which seems to be the best characterized, and for which we provide the most detailed analysis, is one which is reported to be a FM with biaxial anisotropy.

2. Antiferromagnets

It is more difficult to achieve BO's in AFM's because of the local Néel order. We mentioned above that BO's can be

viewed, at least semiclassically, as the result of applying a force on a particle in a band. How can one apply a force to an antiferromagnetic domain wall? The force is given by $\mathbf{F}=-\nabla\Sigma_n \mathbf{b}_n\cdot\mathbf{S}_n$. If the external field $\mathbf{b}$ is homogeneous, then the force quickly averages to zero over the chain. However, applying an *inhomogeneous* field produces a net force. Equation (2) can still be used, but the couplings are now negative, and H^I must be slightly altered to reflect the inhomogeneity of the field:

$$H^I_{\mathrm{AFM}}=|J^z|\sum_n S^z_n S^z_{n+1}-\sum b^z_n S^z_n. \tag{20}$$

The one-soliton states must also be redefined. Rather than Eq. (3), we should write

$$|m,Q\rangle=|\cdots\uparrow\downarrow\overset{m}{\uparrow}\downarrow\downarrow\uparrow\downarrow\uparrow\cdots\rangle. \tag{21}$$

The charge Q can be defined by the first spin at the end of the chain:[11] $Q=-1$ for spin-up, and $Q=+1$ for spin-down. Now it is H^a in Eq. (2c) which will always create additional solitons (and thus should be discarded in the one-soliton approximation). Conversely, $H^\perp$ translates solitons. As a specific example, we can take a magnetic field along the easy axis that linearly increases along the chain axis: $b^z_n=nb^z$ (such a field satisfies Maxwell's equation $\nabla\cdot\mathbf{B}=0$). Projecting down to the one-soliton sector, we obtain

$$H^{\mathrm{AFM}}_{\text{1-sol}}=\frac{|J^z|}{2}+\Delta^{\mathrm{AFM}}(T_2+T_{-2})-\frac{b^zQ}{2}(-1)^m\left(m+\frac{1}{2}\right),$$

$$\Delta^{\mathrm{AFM}}=(J^y+J^x)/4. \tag{22}$$

This Hamiltonian is again similar to Eq. (5). The spectrum again consists of the WZL, but due to the antiferromagnetism, the dependence of the spectrum on the position variable m is slightly altered:

$$E_m=\frac{1}{2}b^z(-1)^m\left(m+\frac{1}{2}\right). \tag{23}$$

The eigenstates are also very similar to Eq. (10). Only α must be slightly changed, again to reflect the antiferromagnetism:

$$\alpha=(-1)^m\frac{J^x+J^y}{2b^z}\quad(Q=-1). \tag{24}$$

Thus, much of what follows applies also to AFM's where the anisotropy can be either uniaxial or biaxial. One must only replace the homogeneous field with a linearly increasing field.

In most of what follows, we shall consider biaxial FM's with static and homogeneous fields. The present subsection, however, shows that the same analysis can be carried over, almost without change, to uniaxial FM's and to biaxial and uniaxial AFM's.

C. Conditions for observation

Here, we briefly touch on the conditions necessary to observe BO's in physical systems. This discussion will have to remain rather vague, as it requires a detailed knowledge of specific material properties and, based on that, further theoretical investigations. Still, we can list a few essential conditions in general terms, which are very similar to the ones studied in the context of mesoscopic effects in electronic systems.[26]

First, there should be no Zener transitions (interband tunneling). The soliton oscillates only when it is reflected from one zone boundary to the opposite one within the same band. If the force on the soliton is too strong, it will gain so much energy at the top of the band that it will tunnel into a higher energy band. This tunneling will produce classical linear motion, rather than the quantum-mechanical BO's. Such transitions can be neglected if the Bloch frequency is much larger than the Zener transition rate. This effectively puts an upper bound on the field driving the particle. In the present context, it means that the exchange constant J^z along the easy axis, a measure of the band gap, should be much larger than the magnetic field b.

Second, there should be no inelastic scattering. Such events occur, for example, by emission and absorption of phonons, or via soliton-soliton interaction. Inelastic scattering may destroy the phase-coherent motion of the particles necessary for BO's to occur. A detailed investigation into the nature and especially the magnitude of the spin-lattice coupling in the spin chains we shall be discussing below is beyond the scope of the present work, and is, in any case, probably a matter best determined experimentally (e.g., from the measured linewidth in the structure factor). It is known, however, that the spin-lattice couplings are far weaker than the analogous charge-lattice couplings. Also, if the soliton density is low enough, soliton-soliton interactions, being typically of short-range nature, can be neglected and the results of band theory are still valid. In Ising-like spin chains, a low-density requirement implies that the temperature should be less than the exchange coupling J_z. Again this can be typically satisfied.

Finally, elastic scattering, such as scattering from static random impurities, may also be a problem (although typically less restrictive). Here, one should consider the Anderson localization length induced by random disorder in low-dimensional systems. This length, which is on the order of the elastic mean free path of the propagating quasiparticle[27] (in the present case, the soliton), should be greater than the Bloch amplitude, which places a lower bound on the B field driving the soliton. However, since the Bloch amplitude can typically be on the order of the lattice constant, this poses no severe constraints.

Although the above conditions are demanding, it is quite encouraging that the presence of extended states of dispersive solitons (i.e., the Villain mode) has been established experimentally in Ising-like antiferromagnets.[16–22] This suggests that, at least for certain spin chains, inelastic scattering and disorder can be neglected to first approximation. In the end, the inelastic mean free time τ_{in} should be compared with the Bloch frequency ω_B. Bloch oscillations are possible if $\omega_B>1/\tau_{\mathrm{in}}$. Typical values for ω_B lie between 40 and 600 GHz (see below).

III. THE DYNAMICAL STRUCTURE FACTOR

In this section, we show that the dynamical structure factor $S^{zz}_b(q,\omega)$ at finite field contains sharp peaks at integer

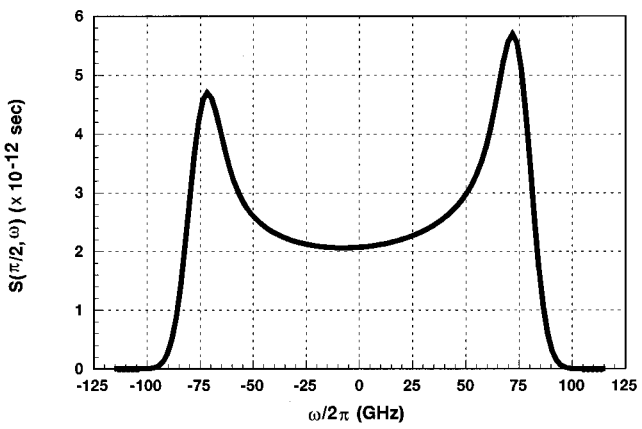

FIG. 2. A plot of $S_0^{zz}(q,\omega)$ for $q=\pi/2$, as given by Eq. (A17), with $\Delta=0.925$ K and $T=18$ K. We have also convoluted $S_0^{zz}(q,\omega)$ with a Gaussian, and so the square-root singularities at $\omega=\pm\Omega_q$ have been rounded, as expected if collisions and interactions are taken into account.

multiples of the Bloch frequency ω_B—clear evidence of the WZL. Thus, inelastic neutron scattering, for example, can detect the WZL. By contrast, we also calculate the dynamical structure factor $S_0^{zz}(q,\omega)$ at zero field and thus give the ferromagnetic analog of the Villain mode for AFM's.

For a translationally invariant system such as the full Hamiltonian in Eq. (2), the dynamical structure factor is defined in the standard way:[28]

$$S^{zz}(q,\omega)=\frac{1}{2\pi}\int_{-\infty}^{\infty}dt\,e^{-i\omega t}\langle\delta S^z_{-q}(0)\,\delta S^z_q(t)\rangle, \quad (25)$$

where $\delta S^z_q=S^z_q-\langle S^z_q\rangle$. The Fourier transform of the spin operator is also defined in the standard way: for a finite chain with $N_{\rm tot}=2N+1$ sites, $S^z_q=\Sigma_{n=-N}^{N}e^{iqn}S^z_n$. (We continue to set $a=1$.) If the eigenbasis $\{|\psi_m\rangle\}$ is orthonormal and discrete, one may write

$$S^{zz}(q,\omega)=\frac{1}{Z}\sum_{m,n}e^{-\beta E_m}|\langle\psi_n|S^z_q|\psi_m\rangle|^2\delta(\omega-E_n+E_m) -|\langle S^z_q\rangle|^2\delta(\omega), \quad (26)$$

where E_m is the energy eigenvalue. In the following subsection, we give results for $b=0$ and later give results for $b\neq 0$.

A. The dispersive mode ($b=0$)

The dynamical structure factor for $b=0$ is calculated in Appendix A. The final expression is given in Eq. (A17) as

$$S_0^{zz}(q,\omega)=\frac{e^{\beta\omega/2}\cosh[(1/2)\,\beta\sqrt{\Omega_q^2-\omega^2}\cot q]}{4\pi\,\sin^2(q/2)I_0(2\Delta\beta)\sqrt{\Omega_q^2-\omega^2}}, \quad (27)$$

where the bandwidth Δ is given in Eq. (5), the cutoff frequency Ω_q in Eq. (A8), and where I_0 is the modified Bessel function of zeroth order. Equation (27) is plotted in Fig. 2 for $\Delta=0.925$ K and $T=18$ K. (These parameters are relevant for the following discussion on the material $CoCl_2\cdot 2H_2O$.) The plot shows the frequency dependence at a fixed wave vector of $\pi/2$. In addition, we have convoluted the dynamical structure factor with a Gaussian $R(\omega)=(1/\sqrt{\pi\sigma})e^{-\omega^2/\sigma}$ with $\sqrt{\sigma}\approx 4$ GHz. Thus, the square-root singularities at $\omega=\pm\Omega_q$ have been rounded, which is the expected effect of soliton-soliton collisions and other interactions we have not taken into account here. This structure factor is very similar to that found in AFM's by Villain[10] and Boucher *et al.*,[17] who also worked in the one-soliton subspace, and by Nagler *et al.*,[18,19] who worked in the two-soliton subspace. As argued by Nagler *et al.*, similar results should be expected for all cases where the soliton number stays fixed.

Equation (A17) assumes the existence of only one soliton in the system, whereas there will always be some finite density of solitons. Since the (thermal) energy required to create a soliton is $J^z/2$, the result in Eq. (A17) may be crudely weighted by a Boltzmann factor given by[17] $S_0^{zz}(q,\omega)\rightarrow e^{-\beta J^z/2}S_0^{zz}(q,\omega)$. A more proper treatment would be to include soliton interaction, with the possibility of creation and annihilation of solitons. Nevertheless, Eq. (A17) should be qualitatively correct for Ising-like FM's just as the antiferromagnetic analog qualitatively describes the experimental findings.

An important difference between the result above for FM's and the result for AFM's is the wave-vector dependence. The factor of $\sin^2(q/2)$ in Eq. (A17) for FM's is replaced by $\cos^2(q/2)$ for AFM's. This difference between sine and cosine is related to the difference in ordering between FM's and AFM's; for AFM's, $q=\pi$ is commensurate with the spatial spin order near the ground state, while for FM's, it is $q=0$ which is commensurate with the ordering. Thus, one can replace q by $\pi-q$ in going from FM's to AFM's; this changes $\sin^2(q/2)$ into $\cos^2(q/2)$. Actually, $\cot q$ and Ω_q also change signs, but Eq. (A17) is invariant under this change. Also, the difference in the bandwidth Δ (J^y+J^x for AFM's and J^y-J^x for FM's) has been discussed in Sec. II B 2.

It should not be so surprising that the result for FM's and AFM's is so similar in the absence of magnetic fields. After all, we have already seen in Sec. II that a variety of Ising-like models gets mapped onto an effective tight-binding model for solitons in the one-soliton approximation. For example, in zero magnetic field, Eq. (5) for FM's is formally identical to Eq. (22) for AFM's. Differences between the two only arise in the presence of a field. But even then, one can choose different field configurations for FM's and AFM's in order to obtain similar structure factors; as shown before, the WZL also exists in AFM's if an inhomogeneous field is applied.

Equation (A17) shows a divergence as $q\rightarrow 0$. This should not be viewed as a physical result, but rather as an indication of the failure of the one-soliton approximation in this limit. In contrast, when we consider the $b\neq 0$ case below, we shall see that the $q\rightarrow 0$ limit is well behaved. This is because the soliton states are now localized and the one-soliton Hamiltonian is no longer translationally invariant on the lattice. (Thus, k is no longer a good quantum number.) This localization should dramatically decrease the collision rate. In this way, the magnetic field provides a physical cutoff for the above singularity at $q=0$. We will come back to this issue in the following subsection.

For an estimate of the soliton-soliton collision rate, we can employ the results in Ref. 17. These authors have looked

at the model described by $H_{\text{1-sol}}^{\text{AFM}}$ in Eq. (22), with $b^z=0$, and so we can use their results for our ferromagnetic model if we simply substitute Δ for Δ^{AFM}. Following Ref. 17, the soliton density is given by $n_s=e^{-\beta J^z/2}$ and the soliton occupation probability by $p(k)=e^{-\beta E(k)}/Z$. The soliton velocity, given by the derivative of the dispersion relation, is $v_k=-4\Delta\sin(2k)$, and the average soliton velocity is defined as $v_0=(1/N_{\text{tot}})\Sigma_k|v_k|p(k)$, whose evaluation yields

$$v_0=\frac{4\sinh(2\Delta\beta)}{\pi\beta I_0(2\Delta\beta)} \overset{2\Delta\beta\ll 1}{\rightarrow} 8\Delta/\pi. \tag{28}$$

The collision rate $\omega_c(k)$ depends on both n_s and v_k, and is given by

$$\omega_c(k)\approx n_s\sum_{k'} p(k')|v_k'-v_k|\approx n_s v_0[1-(1-\pi/2)\sin^2(2k)]. \tag{29}$$

B. The Wannier-Zeeman ladder ($b\neq 0$)

In this subsection, we derive a central result of this paper. In the presence of a magnetic field applied along the Ising axis, the dynamical structure factor will exhibit the signature of the WZL. We shall also find that the $q\rightarrow 0$ limit is well behaved, in contrast to the previous subsection on the zero-field regime. This, together with the fluctuation-dissipation theorem, will also enable us to calculate the uniform susceptibility $\chi''(\omega)$, which provides us with a measure of the magnetization autocorrelation function. We begin first with $S_b^{zz}(q,\omega)$, followed by $\chi''(\omega)$. Most of the technical details are given in Appendix B.

1. The dynamical structure factor

The dynamical structure factor for finite b is calculated in Appendix B. The final expression is given in Eq. (B18) as

$$S_b^{zz}(q,\omega)=\frac{1}{2}\sum_{n=-N}^{N} G_n(q)\,\delta(\omega-n\omega_B), \tag{30a}$$

$$G_0=\frac{J_0^2(\zeta)}{\cosh(\beta\omega_B/2)-\cos q}, \tag{30b}$$

$$G_n=\frac{J_n^2(\zeta)}{2\sin^2(q/2)}\times\begin{cases}1, & n>0\\ e^{n\beta\omega_B}, & n<0,\end{cases} \tag{30c}$$

where $\omega_B=2b$ is the Bloch frequency. Equation (30) indicates in particular that inelastic neutron scattering is capable of *mapping the Wannier-Zeeman ladder*. A soliton initially in some given Wannier-Zeeman state may be excited to higher states. The neutron line-shape intensity for an excitation by n levels, is essentially given by square of the nth order Bessel function $J_n^2(\zeta)$. This means that the *relative amplitudes* of the peaks can be controlled through the argument $\zeta=(2\Delta/b)|\sin q|$ by adjusting the external field b (hence also the Bloch frequency and amplitude). For example, in Figs. 3 and 4, we plot the structure factor as a function of ω for $q=\pi/2$. In these figures, we have convoluted the structure factor with a Gaussian:

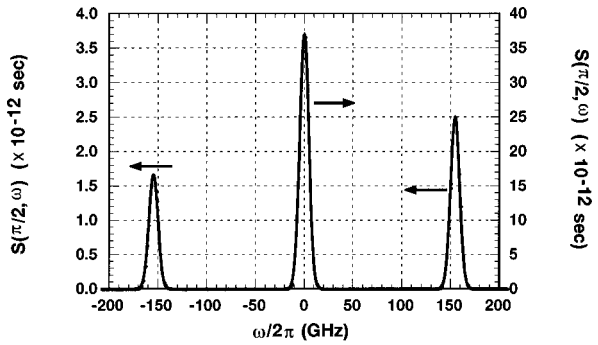

FIG. 3. A plot of Eq. (B18) for $q=\pi/2$, with $A_B=a$ and $\beta\omega_B=0.4$. For the material $CoCl_2\cdot 2H_2O$, this corresponds to an applied field of $H^{\text{tot}}=0.81$ T, $\omega_B/2\pi=154$ GHz, and $T=18$ K. The peaks at $\omega=\pm\omega_B$ are measured on the left vertical axis and the peak at $\omega=0$ is measured on the right. The peaks have been broadened by convoluting with a Gaussian as in Eq. (31), with $\sqrt{\sigma}\approx 40$ GHz.

$$S_b^{zz}(q,\omega)\rightarrow\int_{-\infty}^{\infty} d\omega' R(\omega-\omega')S_b^{zz}(q,\omega'),$$

$$R(\omega)=\frac{1}{\sqrt{\pi\sigma}}e^{-\omega^2/\sigma}. \tag{31}$$

For the plot in Fig. 3, we have taken $T=18$ K, $\Delta=0.925$ K (both as in Fig. 2), and $b=3.71$ K. The choice of these numbers is motivated by the candidate materials to be discussed in the following section. These values give a Bloch frequency of about 154 GHz and a Bloch amplitude of about one lattice constant.[29] For the material $CoCl_2\cdot 2H_2O$ discussed in the following section, this value of b corresponds to an external field of about 0.81 T, and the temperature of 18 K is just above the three-dimensional ordering temperature. In Fig. 4, we use the exact same parameters as in Fig. 3 *except* for b, for which we have set $b=3.71$ K/4 $=0.9275$ K. The Bloch frequency is correspondingly reduced by a factor of 4, while the Bloch amplitude is *in-*

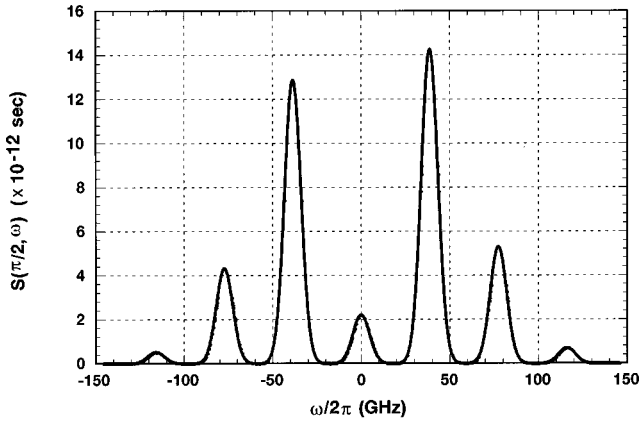

FIG. 4. The same plot as in Fig. 3, but with b reduced by a factor of 4. There is a similar decrease in the Bloch frequency, and a similar *increase* in the Bloch amplitude. The striking feature is the change in the relative amplitudes of the peaks, as compared with Fig. 3. Here we have plotted peaks up to three times the Bloch frequency all on the same scale.

creased by the same factor. The striking feature here is the relative amplitudes of the peaks, as compared with Fig. 3; with this smaller field, peaks up to $\omega=\pm 3\omega_B$ can be distinguished on the same scale. The peaks in both figures away from $\omega=0$ are the signature of the WZL. There exists one peak at every integer multiple of the Bloch frequency, with an amplitude given by the square of a Bessel function.

We have repeated the above calculation numerically (for finite N) and compared the results with the analytic ones just presented. For any given peak at $\omega=n\omega_B$ ($n=0,\pm 1, \pm 2, \ldots$), the numeric results converge to the above analytic ones as the system size $2N+1$ grows. If instead we fix N, then the numeric results converge to the analytic results as one moves away from the boundaries of the chain at $\pm N$. We may thus conclude that the numeric and analytic results agree in the thermodynamic limit.

2. The uniform susceptibility

It is interesting to note that in contrast to the dispersive mode for $b=0$, the $q\to 0$ limit is well behaved when $b\neq 0$:

$$S_b^{zz}(q\to 0,\omega)\to \frac{\delta(\omega)}{4\sinh^2(\beta b/2)} + \left(\frac{\Delta}{b}\right)^2 [\delta(\omega-\omega_B)+e^{\beta\omega}\delta(\omega+\omega_B)]. \tag{32}$$

We have verified this result by performing the calculation at $q=0$ from the outset, as well as by calculating the imaginary part of the zero wave-vector susceptibility $\chi''(\omega)$ in the Matsubara formalism, and then using the fluctuation-dissipation theorem:

$$\chi''(\omega)=\frac{(g\mu_B)^2}{2}(1-e^{-\beta\omega})S_b^{zz}(\omega) = \frac{1}{2}\left(\frac{\Delta}{B}\right)^2(1-e^{-\beta\omega_B})[\delta(\omega-\omega_B)-\delta(\omega+\omega_B)]. \tag{33}$$

Here, we have expressed $\chi''(\omega)$ in units of $\mu_B^2\times$s. Equation (33) represents the response from only one soliton. There should be one such factor for each soliton in the system. Assume, for example, that one soliton exists every ten lattice sites for each chain in the sample. (This requires the Bloch amplitude to be less than ten lattice sites.) A single-crystal of $CoCl_2\cdot 2H_2O$, with a volume of $1\,\mathrm{mm}^3$ will then contain up to 10^{18} solitons. Thus, the signal can be quite large and should thus be observable in standard magnetization measurements (using, for instance, cantilever or superconducting quantum interference device technology).

Again, the structure factor and the susceptibility should be observable as long as the inelastic scattering rate is less than ω_B. Concrete estimates for the soliton collision rate, for example, in the presence of a b field are even more difficult to obtain than for $b=0$. Nevertheless, the rate for sufficiently large b should be far lower than the rate for $b=0$. Indeed, when we turn on the field, the solitons become localized and execute BO's about their mean positions. By tuning the field appropriately, the Bloch amplitude can be kept much smaller than the average distance (i.e., inverse density) between the localized solitons, and in this case the soliton-soliton interaction can be expected to be negligible. We can now go on to compare the zero-field limit of the above ''Wannier-Zeeman'' results with the previous ''dispersive'' results.

C. Discussion of results ($b\to 0$)

As the field decreases, the Bloch amplitude increases. At some point, the Bloch amplitude will be equal to the spacing between solitons in the chain. At this point, collision effects, which are not included in our theory, become important and BO's will be suppressed. This means that, for a meaningful comparison between our approximate theory and experiment, we must consider *either* the zero-field regime ($B=0$), *or* the regime where B is sufficiently large such that our one-soliton approximation is justified.

In this sense, the limit of $B\to 0$ *within* the one-soliton approximation, has no experimental significance. However, it is still interesting from a technical point of view since this limit shows some features reminiscent of the classical limit of a quantum system, in the sense that there might be no *pointwise* convergence.[30] Other well-known examples are the harmonic oscillator and a particle in a linear potential.[30] In general—and especially when interference effects are important, as in the BO problem—some, usually *ad hoc*, averaging procedure must be employed in order to obtain a meaningful classical limit.

The problems show up already at the level of the eigenfunctions and eigenvalues. At finite field, the eigenfunctions are the localized Wannier states (10b), $\langle n|E_m\rangle=[1+(-1)^{m-n})]J_{(m-n)/2}(\alpha)/2$, which satisfy vanishing boundary conditions. But at $b=0$, the extended Bloch states $\langle n|k\rangle = e^{ikn}/\sqrt{N_{\mathrm{tot}}}$ satisfy periodic boundary conditions. It is thus not too surprising that as $b\to 0$, the Wannier states do not converge pointwise to the Bloch states. The same holds for the energy eigenvalues; the band structure cannot be recovered from the WZL in the $b\to 0$ limit.

Similar remarks apply to the partition functions. Keeping a finite system size $N_{\mathrm{tot}}=2N+1$, the partition functions for finite and zero fields are, respectively, given by

$$Z_b=\sum_{m=-N}^{N} e^{-\beta b m}=\frac{\sinh(\beta b N_{\mathrm{tot}}/2)}{\sinh(\beta b/2)}, \tag{34}$$

$$Z_0=\sum_{k=-\pi}^{\pi} e^{-2\Delta\beta\cos(2k)}=N_{\mathrm{tot}}I_0(2\Delta\beta). \tag{35}$$

These expressions imply that the $b\to 0$ limit must be coupled to the $N_{\mathrm{tot}}\to\infty$ limit. For example, if we are in the regime where $\Delta\beta\ll 1$ and $\beta b\ll\beta b N_{\mathrm{tot}}\ll 1$, then to second order in both $\Delta\beta$ and βb, Z_b converges to Z_0 provided we make the identification $bN_{\mathrm{tot}}=2\sqrt{6}\Delta$. On the other hand, if we are in the regime $\Delta\beta\ll 1$ and $\beta b\ll 1\ll\beta b N_{\mathrm{tot}}$, the partition functions cannot be matched.

Next, we look at the dynamical structure factor (B18) which we rewrite here in a slightly different form:

$$S_b^{zz}(q,\omega)=\frac{J^2_{\omega/2b}(\zeta)e^{\beta(\omega-|\omega|)/2}}{4\sin^2(q/2)}\sum_{n=-N}^{N}\delta(\omega-2bn)$$
$$-\frac{J_0^2(\zeta)}{4\sin^2(q/2)}\,\frac{\cosh(\beta b)-1}{\cosh(\beta b)-\cos q}\,\delta(\omega). \tag{36}$$

For $b\to 0$, the second term tends to zero and so we need only concern ourselves with the first term. The Bessel function $J^2_{|\omega|/2b}(\zeta)=J^2_{|\omega|/2b}(|\Omega_q|/2b)$ can be expanded in its asymptotic form for $b\to 0$. If $|\omega|<|\Omega_q|$, then

$$J^2_{|\omega|/2b}\left(\frac{|\Omega_q|}{2b}\right)\approx\frac{4b}{\pi\sqrt{\Omega_q^2-|\omega|^2}}\sin^2\left[\frac{1}{2b}\left(\sqrt{\Omega_q^2-|\omega|^2}\right.\right.$$
$$\left.\left.-|\omega|\arccos\frac{|\omega|}{\Omega_q}\right)+\frac{\pi}{4}\right]. \tag{37}$$

It is the rapidly oscillating factor which prevents the pointwise convergence in the $b\to 0$ limit; some averaging procedure is required. To illustrate this, let us crudely replace the oscillatory factor with 1/2 (which is accurate only for $\omega^2\ll\Omega_q^2$):

$$\overline{J^2_{|\omega|/2b}\left(\frac{|\Omega_q|}{2b}\right)}\approx\frac{2b}{\pi\sqrt{\Omega_q^2-|\omega|^2}}. \tag{38}$$

In the $b\to 0$ limit, the sum over n in Eq. (36) can be made continuous:

$$\sum_{n=-N}^{N}\delta(\omega-2bn)=\frac{1}{2}\sum_{n=-bN}^{bN}\delta\left(\frac{1}{2}\omega-n\right)$$
$$\to\frac{1}{2b}\int_{-bN}^{bN}dn\,\delta\left(\frac{1}{2}\omega-n\right)$$
$$=\begin{cases}1/2b, & |\omega|<2bN\\ 0, & |\omega|>2bN.\end{cases} \tag{39}$$

Inserting Eqs. (38) and (39) into Eq. (36), and assuming $|\omega|<|\Omega_q|$, we can write

$$\lim_{b\to 0}\overline{S_b^{zz}(q,\omega)}\approx\frac{e^{\beta(\omega-|\omega|)/2}}{4\pi\,\sin^2(q/2)\sqrt{\Omega_q^2-\omega^2}}\neq S_0^{zz}(q,\omega). \tag{40}$$

Although the last two expressions are not equal, they are nevertheless quite similar. In Fig. 5, we plot the two results, Eqs. (40) and (A17), using the same parameters as in the previous figures. The small deviations can be traced back to the rapidly oscillating sine squared function in Eq. (37). We have replaced this by the constant factor of 1/2. This is not quite proper since the period of the oscillation is a function of ω (and not just a constant). Near the cutoff frequency Ω_q, this error becomes the most apparent because the rest of the function in Eq. (37) is also a rapidly varying function (it is tending to a square-root singularity). In the inset of Fig. 5, we have plotted the ratio

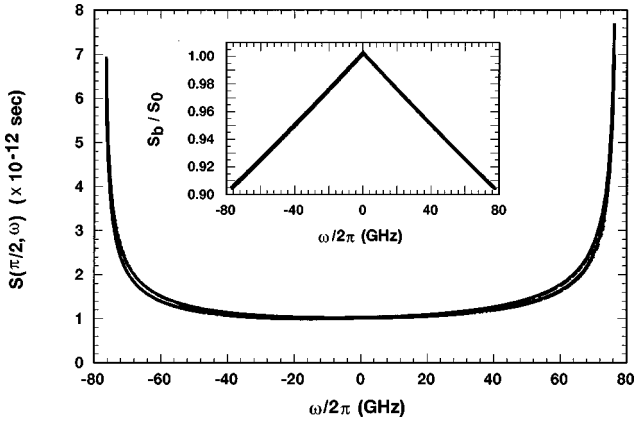

FIG. 5. A plot of both $\lim_{b\to 0}S_b^{zz}(\pi/2,\omega)$ in Eq. (40), and $S_0^{zz}(\pi/2,\omega)$ in Eq. (A17). Good agreement is obtained, but there is some discrepancy as shown in the inset, which shows the ratio of the two functions (41). This should be a constant (equal to one) if the two results are the same. The source of this discrepancy is discussed in the text.

$$\frac{\lim_{b\to 0}\overline{S_b^{zz}(\pi/2,\omega)}}{S_0^{zz}(\pi/2,\omega)}\approx\frac{e^{-\beta|\omega|/2}I_0(2\Delta\beta)}{\cosh[(1/2)\,\beta\sqrt{\Omega_q^2-\omega^2}\cot q]}, \tag{41}$$

as a function of ω for the same values of Δ, β, and q used in previous plots. Near $\omega=0$ the agreement is best (the ratio is near unity). But as $\omega\to\Omega_q$, the agreement becomes progressively worse. Nevertheless, this rather crude treatment achieves reasonable agreement—only about 10% error at its worst. The agreement improves if we choose $q\neq\pi/2$, but worsens as the product $\Delta\beta$ grows. (But $\Delta\beta\ll 1$ is the regime of interest.)

This marks the end of the theoretical development. In the following section, we shall concentrate on various materials we believe are good candidates for observing the WZL. Specifically, we shall see that BO's can exist in certain ferromagnetic Ising-like salts, with frequencies on the order of 150 GHz.

IV. CANDIDATE MATERIALS

We have identified four candidate materials for observing BO's and the WZL in purely magnetic systems. The materials are all Ising-like FM's, and consist of chains of magnetic ions, with effective spin-$\frac{1}{2}$, separated by spacer material. We focus mainly on $CoCl_2\cdot 2H_2O$ (Ref. 12), but give also a brief discussion on the potentially more promising, but less well characterized, $CoCl_2\cdot 2NC_5H_5$ (Ref. 31), $[(CH_3)_3NH]CoCl_3\cdot 2H_2O$ (Ref. 32), and $[(CH_3)_3NH]FeCl_3\cdot 2H_2O$ (Ref. 33).

A. $CoCl_2\cdot 2H_2O$

In $CoCl_2\cdot 2H_2O$, the magnetic Co ions form chains along the c axis. The coupling is ferromagnetic between ions in the same chain (we consider interchain exchange below). The exchange anisotropy is such that the b axis is an easy axis. The work of Ref. 12 confirms unambiguously that the Ising-like spin-$\frac{1}{2}$ Hamiltonian of Eq. (2) describes this system very well. In Table I, we list the material parameters of this fer-

TABLE I. Relevant parameters for the candidate materials discussed in the text. A dashed entry (—) means that no value was given in the references.

Parameter	Value			
	CCH[a]	CCN[b]	CoTAC[c]	FeTAC[d]
J^z	18.3 K	10 K	14.2 K	17.4 K
J^y-J^x	3.7 K	—	—	—
J^y+J^x	5.6 K	—	—	—
J_1^z	−4.6 K	−3.4 K	0.18 K	−0.02 K
J_2^z	−0.9 K	—	-10^{-3} K	0.00 K
a	3.55 Å	3.66 Å	3.63 Å	3.68 Å
g	6.81	5.49	6.54	7.49
T_{3D}	17.2 K	3.17 K	4.14 K	3.12 K

[a] $CoCl_2\cdot 2H_2O$ (Ref. 12).
[b] $CoCl_2\cdot 2NC_5H_5$ (Ref. 31).
[c] $[(CH_3)_3NH]CoCl_3\cdot 2H_2O$ (Ref. 32).
[d] $[(CH_3)_3NH]FeCl_3\cdot 2H_2O$ (Ref. 33).

romagnetic salt. (We have taken the crystal b axis to coincide with the z axis of the Cartesian coordinate frame.) We also list two antiferromagnetic interchain couplings. (We follow Ref. 12 in neglecting the small non-Ising part of the interchain exchange.) We shall consider this interchain coupling in a mean-field treatment by considering the total field at a given site to be the sum of the externally applied field and some internal field due to interchain exchange.

Let us first neglect the interchain interaction and consider just a single chain in the presence of a static and homogeneous field along the z axis. Then, the one-soliton approximation should be valid if the external field $b^z=g\mu_B H_{\rm ext}^z$ is less than the Ising exchange coupling J^z. For the parameters given in Table I, this puts a restriction on the field strength of $H_{\rm ext}^z<4$ T. For example, if we apply a 0.81 T field—comfortably below this upper bound—then the Bloch amplitude and frequency are given from Eq. (9) as

$$A_B=a\frac{J_y-J_x}{g\mu_B H_{\rm ext}^z}\approx a,\quad \frac{\omega_B}{2\pi}=\frac{g\mu_B H_{\rm ext}^z}{\hbar\pi}\approx 154\ \text{GHz}. \tag{42}$$

This amplitude is small enough to impede the destructive influence of any scattering events, and the frequency falls within the capabilities of neutron scattering. This is therefore an encouraging result.

Due to the antiferromagnetic interchain couplings J_1^z and J_2^z, the material undergoes a three-dimensional ordering transition at about 17 K. Below this temperature, and in zero external field, there still exists ferromagnetic order within each chain, but the chains are ordered antiferromagnetically with respect to each other. As the field is turned on there are successive transitions from antiferromagnetic, to ferrimagnetic, and finally to ferromagnetic order at fields H_{c1} and H_{c2}, respectively. At all times, the intrachain order is ferromagnetic. This is depicted in Fig. 6, where we also list the interchain coupling values[12] and the critical fields.[34,12] When determining the Bloch amplitude and frequency, one should also include these internal fields. For example, a Bloch amplitude of one lattice constant, which results from a *total*

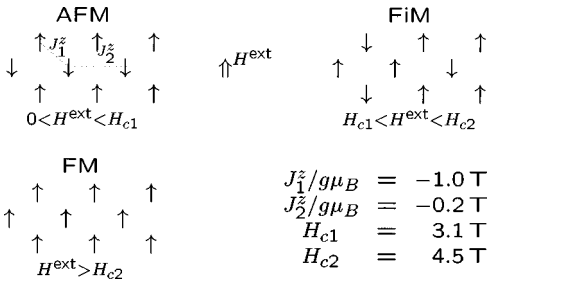

FIG. 6. The three phases of $CoCl_2\cdot 2H_2O$ for $T<17.2$ K. The spin chains run perpendicular to the page and J_1^z and J_2^z are the interchain antiferromagnetic couplings. These couplings can be considered internal fields, and so they too affect the Bloch oscillations. In fact, Bloch oscillations can potentially exist in all three phases. This figure has been adapted from Ref. 12.

field of $H_{\rm tot}=0.81$ T, can be realized in all three phases when these internal fields are taken into account. Explicitly, we have (for $H_{\rm tot}=0.81$ T)

$$\text{AFM:}\quad H_{\downarrow}^{\rm tot}=-H^{\rm ext}-4J_1^z/g\mu_B+2J_2^z/g\mu_B\Rightarrow H^{\rm ext}=2.8\ \text{T}, \tag{43a}$$

$$\text{FIM:}\quad H_{\downarrow}^{\rm tot}=-H^{\rm ext}-4J_1^z/g\mu_B-2J_2^z/g\mu_B\Rightarrow H^{\rm ext}=3.6\ \text{T}, \tag{43b}$$

$$\text{FM:}\quad H_{\uparrow}^{\rm tot}=H^{\rm ext}+4J_1^z/g\mu_B+2J_2^z/g\mu_B\Rightarrow H^{\rm ext}=5.2\ \text{T}. \tag{43c}$$

The notation $H_{\downarrow}^{\rm tot}$, for example, denotes the total field at a chain with spin down, where ''down'' is defined as being opposite to the external field. Thus, in the ferromagnetic phase, all chains are spin up. In Fig. 7 we plot the resulting predictions for the Bloch frequency and (inverse) Bloch amplitude as a function of external field in all three phases. The antiferromagnetic and ferrimagnetic phases show two curves because these phases have both spin-up and spin-down chains, and these chains each feel a different field. The dotted horizontal lines are bounds, outside of which the results become equivocal; near the upper bound, the total field be-

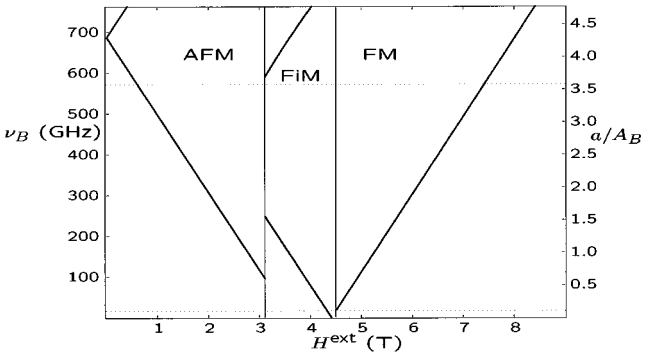

FIG. 7. A plot of Bloch frequency and inverse Bloch amplitude in $CoCl_2\cdot 2H_2O$ as a function of external field below the three-dimensional ordering temperature of about 17 K. The discontinuous jumps in the curves are a result of transitions from anti-, to ferri-, and finally to ferromagnetic order of the chains relative to each other. Ferromagnetic order is always maintained *within* each chain. The horizontal dotted lines denote upper and lower bounds, beyond which the present analysis should not be expected to hold.

comes comparable to the Ising exchange constant J^z; near the lower bound, the amplitude becomes too large, so that scattering effects should probably be taken into account. There is however, a fairly large intermediate range of over 400 GHz where the effect should be noticeable.

B. Other materials

Another material we wish to mention here is $CoCl_2 \cdot 2NC_5H_5$ (Ref. 31). This material differs from the one above only by the spacer material—pyridine molecules rather than water. Pyridine is a larger molecule than water and so the magnetic chains are further apart by about a factor of 1.7 (9.4 Å versus 5.5 Å for the water spacer). This material is thus a better one-dimensional material than $CoCl_2 \cdot 2H_2O$. The three-dimensional ordering temperature is about 5.4 times smaller than it is in $CoCl_2 \cdot 2H_2O$ (3.17 K rather than 17 K). The material parameters are summarized in Table I. Because the experimental work on this material seems less extensive than that on $CoCl_2 \cdot 2H_2O$, we have not made any predictions for BO's in this material. But due to the reduced three-dimensional ordering temperature, this material should be a better candidate for observing BO's and the WZL. Even if there really is no transverse anisotropy ($J_y = J_x$), BO's could still be induced by simply applying a transverse field in addition to the one along the Ising axis (see Sec. II B 1).

Most of the preceding paragraph applies even more emphatically to the final two materials listed in Table I, particularly to FeTAC.[33] The small magnitude of the interchain couplings and the lower three-dimensional ordering temperature indicate that these materials may be quite suitable for BO's. We have again chosen not to provide predictions for this compound since we believe further material characterization is necessary.

In summary, we have shown in this section that there are a number of materials which may exhibit a dispersive soliton mode as well as BO's. We have not discussed any AFM chains because we have been unable to identify any with the appropriate material parameters such that the Bloch frequency and amplitude fall within experimentally accessible regimes. Should any such chains exist, Sec. II B 2 shows that BO's may exist under an applied inhomogeneous magnetic field.

V. SUMMARY AND OUTLOOK

In this work, we have shown that BO's of magnetic solitons occur in anisotropic spin-$\frac{1}{2}$ chains. Although we have focused primarily on biaxial Ising-like FM's, we have shown that BO's can also occur in uniaxial FM's by applying a transverse field in addition to the longitudinal field. We have also shown that BO's may exist in Ising-like AFM's by applying an inhomogeneous field.

We have been mainly envisioning a neutron-scattering experiment in this work because the dynamical structure factor shows clear evidence of the WZL; it contains sharp peaks at integer multiples of the Bloch frequency. At zero wave vector, all the peaks vanish except for the one at zero frequency and those at the Bloch frequency $\pm \omega_B$. Thus, a measurement of the magnetization autocorrelation function (magnetic susceptibility) about the Bloch frequency should also detect the WZL.

Several materials are promising candidates for observing BO's and the WZL. We have chosen to focus our estimates on the one-dimensional salt $CoCl_2 \cdot 2H_2O$. Although this material is not an ideal one-dimensional substance (better ones have been identified above), BO's of amplitude one lattice constant (about 3.6 Å) and frequency of about 154 GHz are possible with applied fields of a few Tesla. The other materials we have mentioned are less well characterized than the one just described. However, the much smaller interchain coupling indicates that they are better one-dimensional samples—a statement further supported by their three-dimensional ordering temperature, which is much lower than $CoCl_2 \cdot 2H_2O$. It is possible that these materials contain only uniaxial anisotropy. If so, BO's can be achieved by tilting the external field away from the Ising axis.

A question we are currently investigating is what effect soliton-soliton interactions have on the WZL, as well as the related question on the influence of the higher-soliton states. The WZL and BO's should survive if the number of solitons is conserved. In Ref. 19, a study is presented of soliton dynamics in the two-soliton sector (but in zero applied field). If one enforces periodic boundary conditions, then only even numbers of solitons can exist. But quantities calculated in the thermodynamic limit should be independent of the boundary conditions employed. Therefore, as expected, this work found practically the same result for the dynamical structure factor as Villain did working in the one-soliton sector. However, the two-soliton sector brings with it an opportunity to directly detect the *coherent oscillation of solitons*. For example, two solitons can form a bound state which should be identified as a magnon in spin-$\frac{1}{2}$ chains. Multiple magnon bound states can then be formed in which a cluster of adjacent spins are all flipped relative to the majority of the ferromagnetically aligned spins in the chain. Indeed, these are precisely the excitations measured in the work of Ref. 12 which concerns the optical excitation of multiple-magnon bound states. An enticing scenario exists if the ends of these clusters also undergo Bloch oscillation. Rather than having these excitations thermally created, as we have been assuming above, one can then optically create these excitations *coherently* by infrared radiation. The resulting Bloch oscillations will then also be coherent, and this may be detected, for example, by looking for coherent emission of magnetic dipole radiation in the microwave regime. In this scenario, the magnetic Bloch oscillator is an emitter of coherent microwave radiation. This is essentially the analog of the electronic BO experiments, where the charge carriers are optically excited with visible light, and the electron dipole oscillations radiate in the submillimeter regime. There are no exciton effects in our spin chains and so the detection of the magnetic radiation would be a clear signal of magnetic Bloch oscillations. This intriguing problem will be the subject of a future publication.

ACKNOWLEDGMENTS

We thank Guido Burkard, Alain Chiolero, Jack Harris, Bruce Normand, and Eugene Sukhorukov for discussion and helpful comments. We also acknowledge the hospitality of

the ITP, Santa Barbara, where the initial stage of this work was completed. This work was funded by the Swiss NSF, the U.S. NSF under Grant No. PHY94-07194, and the Canadian NSERC.

APPENDIX A: THE DYNAMICAL STRUCTURE FACTOR IN ZERO FIELD

Without a magnetic field, the eigenstates are the Bloch states Eq. (6). Substituting these states, for a fixed charge of $Q=-1$, into Eq. (26) yields

$$S_0^{zz}(q,\omega)=\frac{1}{Z}\sum_{k,k'} e^{-\beta E(k)}|\langle k'|S_q^z|k\rangle|^2 \times\delta(\omega-E(k')+E(k))-|\langle S_q^z\rangle|^2\delta(\omega), \tag{A1}$$

where $E(k)$ is shown in Eq. (7). (We neglect the constant factor of $J^z/2$ since it drops out in the end.) The partition function Z can be expressed in terms of the modified Bessel function of order zero:

$$Z=\sum_k e^{-\beta E(k)}=N_{\rm tot}I_0(2\Delta\beta). \tag{A2}$$

The matrix elements of S_q^z in the eigenbasis can be found by first noting that

$$S_n^z|m\rangle=\begin{cases}-(1/2)|m\rangle, & m\geqslant n\\ (1/2)|m\rangle, & m<n,\end{cases} \tag{A3}$$

from which it follows that

$$S_n^z|k\rangle=\frac{1}{2}|k\rangle-\frac{1}{\sqrt{N_{\rm tot}}}\sum_{m=n}^{N} e^{ikm}|m\rangle. \tag{A4}$$

The one-soliton approximation breaks down as $q\to 0$.[10,19,17] If the neutron transfers no momentum to the system, then the energy will likely go into the creation of another soliton (actually a soliton-antisoliton pair). These are not the processes we are interested in here and are not contained in our approximation. Rather, we wish to consider the process where a neutron *scatters* the soliton from one k state to another, which is less and less likely to happen as $q\to 0$. Below, we shall give estimates of both the soliton density and collision rate.

Limiting the discussion to $q\neq 0$, the matrix elements of S_q^z are given by $\langle k'|S_q^z|k\rangle=(e^{iq}\delta_{k',k+q}-e^{-iqN}\delta_{kk'})/(1-e^{iq})$, and so the modulus squared becomes

$$|\langle k'|S_q^z|k\rangle|^2=\frac{1}{4\sin^2(q/2)}(\delta_{k',k+q}+\delta_{kk'}). \tag{A5}$$

From this, we can find the first term in Eq. (A1):

$$S_0^{zz}(q,\omega)+|\langle S_q^z\rangle|^2\delta(\omega) =\frac{1}{4\sin^2(q/2)}\left(\delta(\omega)+\frac{1}{Z}\sum_k e^{-\beta E(k)} \times\delta(\omega-E(k+q)+E(k))\right). \tag{A6}$$

The Dirac delta function can be written as

$$\delta(\omega-E(k+q)+E(k))=\delta(\omega+\Omega_q\sin(2k+q)), \tag{A7}$$

$$\Omega_q=4\Delta\sin q, \tag{A8}$$

where Ω_q represents an upper bound or cutoff on the frequency. Above this frequency, the structure factor vanishes. This is a direct result of the one-soliton approximation, which yields a dispersion relation with a *finite* bandwidth. For a given momentum transfer q, the maximum energy a soliton can absorb (or emit), while still remaining in the same band, is Ω_q. The δ function (A7) can be written in a more usable form by using the relation $\delta(f(k))=\Sigma_n\delta(k-k_n)/|f'(k_n)|$, where the k_n are the zeroes of $f(k)$. In our case, $f'(k)=2\Omega_q\cos(2k+q)$ and the k_n are fixed by the condition

$$\sin(2k_n+q)=-\omega/\Omega_q. \tag{A9}$$

If we substitute these results into Eq. (A6), and in addition take the continuum limit ($\Sigma_k\to N_{\rm tot}\int dk/2\pi$ and $N_{\rm tot}\to\infty$), we obtain

$$S_0^{zz}(q,\omega)+|\langle S_q^z\rangle|^2\delta(\omega) =\frac{1}{4\sin^2(q/2)}\left(\delta(\omega)+\frac{N_{\rm tot}}{2\pi Z}\sum_n\frac{e^{-2\beta\Delta\cos(2k_n)}}{|2\Omega_q\cos(2k_n+q)|}\right). \tag{A10}$$

To perform the sum over n, we must first solve Eq. (A9). Defining $\omega/\Omega_q\equiv\sin\phi$, where $|\phi|\leqslant\pi/2$ since $|\omega|\leqslant|\Omega_q|$, Eq. (A9) is rewritten as $\sin(2k_n+q)=-\sin\phi$. The general solution is

$$2k_n+q=(-1)^{n+1}(n\pi+\phi), \tag{A11}$$

which is valid for arbitrary integer n ($n=0,\pm1,\pm2,\ldots$). But not all values of n are allowed; the allowed values of n must be chosen such that $|k_n|\leqslant\pi$, implying that the allowed values of n depend on the values of both ϕ and q, where $|\phi|\leqslant\pi/2$ and $|q|\leqslant\pi$. For example, $n=0$ is always allowed, $n=-3$ is allowed only if $\pi\leqslant(\phi-q)\leqslant 3\pi/2$, and $|n|\geqslant 4$ is never allowed. It turns out that for any ϕ and q, there are always four values of n which are allowed—two even values (either $n=0,2$ or $n=0,-2$) and two odd values (either $n=1,3$, $n=\pm1$, or $n=-1,-3$). Actually, the specific value of n makes no difference; the important point is whether n is even or odd (and there are always two of each allowed). For example, from Eq. (A11) we can write

$$|2\Omega_q\cos(2k_n+q)|=|(-1)^n 2\Omega_q\cos\phi|=2\sqrt{\Omega_q^2-\omega^2}. \tag{A12}$$

Similarly, we have

$$-2\Delta\beta\cos(2k_n)$$
$$=-2\Delta\beta[(-1)^n\cos\phi\cos q-\sin\phi\sin q]$$
$$=\frac{\beta}{2}[\pm(-1)^{n+1}\sqrt{\Omega_q^2-\omega^2}\cot q+\omega], \qquad \text{(A13)}$$

where the top sign $(+)$ is for $|q|\leqslant\pi/2$, and the bottom sign $(-)$ for $\pi/2<|q|\leqslant\pi$. (These signs will also prove irrelevant.) We can use the above two results to write the sum in Eq. (A10) as

$$\sum_n \frac{e^{-2\beta\Delta\cos(2k_n)}}{|2\Omega_q\cos(2k_n+q)|}$$
$$=\frac{1}{2\sqrt{\Omega_q^2-\omega^2}}\sum_n \exp\left[\frac{1}{2}\beta[\pm(-1)^{n+1}\times\sqrt{\Omega_q^2-\omega^2}\cot q+\omega]\right]. \qquad \text{(A14)}$$

We see now that the magnitude of n plays no role; it only matters whether n is even or odd. Since there are always two even and two odd values of n, the sum over the exponential becomes a hyperbolic cosine, and therefore the additional $\pm$ also becomes irrelevant:

$$\sum_n \exp\left[\frac{1}{2}\beta[\pm(-1)^{n+1}\sqrt{\Omega_q^2-\omega^2}\cot q+\omega]\right]$$
$$=4e^{\beta\omega/2}\cosh\left(\frac{1}{2}\beta\sqrt{\Omega_q^2-\omega^2}\cot q\right). \qquad \text{(A15)}$$

Gathering the above results, the structure factor becomes

$$S_0^{zz}(q,\omega)+|\langle S_q^z\rangle|^2\delta(\omega)$$
$$=\frac{1}{4\sin^2(q/2)}\times\left(\delta(\omega)+\frac{e^{\beta\omega/2}\cosh[(1/2)\beta\sqrt{\Omega_q^2-\omega^2}\cot q]}{\pi I_0(2\Delta\beta)\sqrt{\Omega_q^2-\omega^2}}\right). \qquad \text{(A16)}$$

For the calculation of $|\langle S_q^z\rangle|^2$, we proceed by noting that, for $q\neq 0$, $\langle k|S_q^z|k\rangle=-e^{-iqN}/(1-e^{iq})$. Since this is independent of k, we have $|\langle S_q^z\rangle|^2=|\langle k|S_q^z|k\rangle|^2=1/4\sin^2(q/2)$. Finally, subtracting this from Eq. (A16), we obtain $S_0^{zz}(q,\omega)$:

$$S_0^{zz}(q,\omega)=\frac{e^{\beta\omega/2}\cosh[(1/2)\beta\sqrt{\Omega_q^2-\omega^2}\cot q]}{4\pi\sin^2(q/2)I_0(2\Delta\beta)\sqrt{\Omega_q^2-\omega^2}}. \qquad \text{(A17)}$$

APPENDIX B: THE DYNAMICAL STRUCTURE FACTOR IN A FINITE FIELD

Using the eigenbasis of Eq. (10) we can write the dynamical structure factor (26) as[35]

$$S_b^{zz}(q,\omega)=Z^{-1}\sum_{m,n=0}^{2N} e^{-\beta bm}|\langle E_{n-N}|S_q^z|E_{m-N}\rangle|^2\times\delta(\omega-b(n-m))-|\langle S_q^z\rangle|^2\delta(\omega). \qquad \text{(B1)}$$

Here, we have shifted the origin of our coordinates to one end of the chain (with a similar shift in the partition function Z). Because of the simple energy-level structure Eq. (12), the partition function is simply given by

$$Z=\frac{1-e^{-\beta bN_{\rm tot}}}{1-e^{-\beta b}}\underset{\beta bN_{\rm tot}\gg 1}{\rightarrow}\frac{1}{1-e^{-\beta b}}. \qquad \text{(B2)}$$

We shall assume $\beta bN_{\rm tot}\gg 1$ in all that follows.

To obtain the matrix elements of S_q^z, note first that from Eqs. (A3) and (10), it follows that

$$S_n^z|E_m\rangle=\frac{1}{2}\left(|E_m\rangle-2\sum_{m'=n}^{N} C_{mm'}|m'\rangle\right). \qquad \text{(B3)}$$

Using this, along with the relations $\langle E_m|m'\rangle=C_{mm'}$ and $\langle E_m|E_{m'}\rangle=\delta_{mm'}$, we can find the matrix elements of S_q^z:

$$\langle E_{\bar m}|S_q^z|E_m\rangle=\frac{N_{\rm tot}\delta_{\bar m m}\delta_{q0}}{2}-\sum_{n=-N}^{N} e^{iqn}\sum_{m'=n}^{N} C_{\bar m m'}C_{mm'}. \qquad \text{(B4)}$$

The expansion coefficients C_{mn} are given in Eq. (10b). The second term on the right side can be brought into a more manageable form by interchanging the order of the summations:

$$\sum_{n=-N}^{N} e^{iqn}\sum_{m'=n}^{N} C_{\bar m m'}C_{mm'}=\sum_{m'=-N}^{N} C_{\bar m m'}C_{mm'}\sum_{n=-N}^{m'} e^{iqn}. \qquad \text{(B5)}$$

Performing the geometric sum over the exponential, the right side is rewritten as

$$\frac{1}{1-e^{iq}}\sum_{m'=-N}^{N}(e^{-iqN}-e^{iq(m'+1)})C_{\bar m m'}C_{mm'}$$
$$=\frac{1}{1-e^{iq}}\left(\frac{1+(-1)^{\bar m-m}}{2}\right)\times\sum_{m'=(m-N)/2}^{(m+N)/2}(e^{-iqN}-e^{iq(m+1-2m')})\times J_{m'}(\alpha)J_{m'+(\bar m-m)/2}(\alpha). \qquad \text{(B6)}$$

For $N\rightarrow\infty$ (but keeping m finite for now), the sum over the product of Bessel functions can be performed using the identity[24]

$$\sum_{k=-\infty}^{\infty} J_k(r)J_{k+n}(\rho)\begin{Bmatrix}\sin\\ \cos\end{Bmatrix}(k\varphi)=J_n(R)\begin{Bmatrix}\sin\\ \cos\end{Bmatrix}(n\vartheta), \qquad \text{(B7)}$$

where, for all variables real and for n an integer, R and ϑ are defined through the relations $R=\sqrt{r^2+\rho^2-2r\rho\cos\varphi}$, $R\cos\vartheta=\rho-r\cos\varphi$, and $R\sin\vartheta=r\sin\varphi$. In particular,

$$\sum_{m'=-\infty}^{\infty} e^{-2iqm'}J_{m'}(\alpha)J_{m'+(\bar{m}-m)/2}(\alpha) = (-i\ \mathrm{sgn}\,q)^{(\bar{m}-m)/2}e^{iq(\bar{m}-m)/2}J_{(\bar{m}-m)/2}(2\alpha|\sin q|). \tag{B8}$$

Now we can substitute Eqs. (B6) and (B8) into Eq. (B4), which enables us to write the matrix elements in closed form as

$$\langle E_{\bar{m}}|S_q^z|E_m\rangle=\left(\frac{1}{2}N_{\mathrm{tot}}\delta_{q0}-\frac{e^{-iqN}}{1-e^{iq}}\right)\delta_{\bar{m}m} -\frac{1+(-1)^{\bar{m}-m}}{2}(-i\ \mathrm{sgn}\ q)^{(\bar{m}-m)/2} \times\frac{e^{iq(\bar{m}+m)/2}}{1-e^{-iq}}J_{(\bar{m}-m)/2}(\zeta), \tag{B9}$$

where $\zeta=(2\Delta/b)|\sin q|$.

Taking the modulus squared and shifting the origin as in Eq. (B1), we can evaluate the first term in the dynamical structure factor:

$$S_b^{zz}(q,\omega)+|\langle S_q^z\rangle|^2\delta(\omega) =\left(\frac{1}{4}N_{\mathrm{tot}}-1-\frac{1}{Z}\sum_{m=0}^{2N}me^{-\beta bm}\right)N_{\mathrm{tot}}\delta_{q0}\delta(\omega) +\left(\frac{1}{2}-J_0(\zeta)\frac{1}{Z}\sum_{m=0}^{2N}\cos[q(m+1)]e^{-\beta bm}\right) \times\frac{\delta(\omega)}{2\sin^2(q/2)}+\frac{J_{\omega/2b}^2(\zeta)}{4\sin^2(q/2)}\frac{1}{Z} \times\sum_{m,n=0}^{2N}{}'e^{-\beta bm}\delta(\omega-b(n-m)). \tag{B10}$$

The prime on the final summation indicates that only those terms with $m-n$ even should be included. The first of three sums in Eq. (B10) is proportional to the derivative of the partition function:

$$\frac{1}{Z}\sum_{m=0}^{2N}me^{-\beta bm}=-\frac{1}{b}\frac{\partial}{\partial\beta}\ln Z=\frac{1}{e^{\beta b}-1}. \tag{B11}$$

The second sum in Eq. (B10) can be written as a geometric series by writing the cosine as an exponential. The result is

$$\frac{1}{Z}\sum_{m=0}^{2N}\cos[q(m+1)]e^{-\beta bm}=\frac{(\cos q-e^{-\beta b})(1-e^{-\beta b})}{|e^{-iq}-e^{-\beta b}|^2}, \tag{B12}$$

For the third and final sum in Eq. (B10), progress can be made by breaking it up into one containing terms with n and m even, and another containing terms with n and m odd; for the odd sums, we set $n\to 2n+1$ and $m\to 2m+1$, and for the even sums, $n\to 2n$ and $m\to 2m$. If we then recombine these two sums, and in addition take $\nu\equiv n-m$, the final sum in Eq. (B10) can be written as

$$\sum_{m,n=0}^{2N}{}'e^{-\beta bm}\delta(\omega-b(n-m)) \to(1+e^{-\beta b})\sum_{m=0}^{N}e^{-2\beta bm}\sum_{\nu=-m}^{N-m}\delta(\omega-2b\nu). \tag{B13}$$

Now we can interchange the order of the sums by using the identity

$$\sum_{m=0}^{N}e^{-2\beta bm}\sum_{\nu=-m}^{N-m}\delta(\omega-2b\nu) =\sum_{\nu=-N}^{0}\delta(\omega-2b\nu)\sum_{m=-\nu}^{N}e^{-2\beta bm}+\sum_{\nu=1}^{N}\delta(\omega-2b\nu) \times\sum_{m=0}^{N-\nu}e^{-2\beta bm}. \tag{B14}$$

The geometric sums can now be performed. Using also the fact that $\beta bN\gg 1$, Eq. (B13) is written as

$$\sum_{m,n=0}^{2N}{}'e^{-\beta bm}\delta(\omega-b(n-m)) =Ze^{\beta(\omega-|\omega|)/2}\sum_{n=-N}^{N}\delta(\omega-2bn). \tag{B15}$$

Substituting Eqs. (B11), (B12), and (B15) into Eq. (B10) yields

$$S_b^{zz}(q,\omega)+|\langle S_q^z\rangle|^2\delta(\omega) =\left(\frac{1}{4}N_{\mathrm{tot}}-\frac{1}{1-e^{-\beta b}}\right)N_{\mathrm{tot}}\delta_{q0}\delta(\omega) +\left(\frac{1}{2}-J_0(\zeta)\frac{(\cos q-e^{-\beta b})(1-e^{-\beta b})}{|e^{-iq}-e^{-\beta b}|^2}\right) \times\frac{\delta(\omega)}{2\sin^2(q/2)}+\frac{e^{\beta(\omega-|\omega|)/2}J_{\omega/2b}^2(\zeta)}{4\sin^2(q/2)}\sum_{n=-N}^{N}\delta(\omega-2bn). \tag{B16}$$

The last term is the most interesting one; it will induce transitions between Wannier-Zeeman levels. Let us first, however, complete the calculation by determining $|\langle S_q^z\rangle|^2$. From Eqs. (B2) and (B9), we have

$$|\langle S_q^z\rangle|^2=\left|\frac{N_{\rm tot}\delta_{q0}}{2}-\frac{e^{-iqN}}{1-e^{iq}}\left(1-J_0(\zeta)\frac{1-e^{-\beta b}}{e^{-iq}-e^{-\beta b}}\right)\right|^2$$
$$=N_{\rm tot}\delta_{q0}\left(\frac{1}{4}N_{\rm tot}-\frac{1}{1-e^{-\beta b}}\right)$$
$$+\left(1-2J_0(\zeta)\frac{(\cos q-e^{-\beta b})(1-e^{-\beta b})}{|e^{-iq}-e^{-\beta b}|^2}\right.$$
$$\left.+J_0^2(\zeta)\frac{\cosh(\beta b)-1}{\cosh(\beta b)-\cos q}\right)\frac{1}{4\sin^2(q/2)}. \quad \text{(B17)}$$

Finally, from Eqs. (B16) and (B17) we obtain the dynamical structure factor:

$$S_b^{zz}(q,\omega)=\frac{1}{2}\sum_{n=-N}^{N}G_n(q)\,\delta(\omega-n\omega_B), \quad \text{(B18a)}$$

$$G_0=\frac{J_0^2(\zeta)}{\cosh(\beta\omega_B/2)-\cos q}, \quad \text{(B18b)}$$

$$G_n=\frac{J_n^2(\zeta)}{2\sin^2(q/2)}\times\begin{cases}1, & n>0\\ e^{n\beta\omega_B}, & n<0,\end{cases} \quad \text{(B18c)}$$

where $\omega_B=2b$ is the Bloch frequency.

*Electronic address: kyriakidis@ubaclu.unibas.ch
†Electronic address: loss@ubaclu.unibas.ch

[1] F. Bloch, Z. Phys. **52**, 555 (1928); C. Zener, Proc. R. Soc. London, Ser. A **145**, 523 (1934).
[2] G. H. Wannier, Rev. Mod. Phys. **34**, 645 (1962).
[3] O. Madelung, *Introduction to Solid-State Theory* (Springer, Berlin, 1981).
[4] J. Feldmann, K. Leo, J. Shah, D. A. B. Miller, J. E. Cunningham, T. Meier, G. von Plessen, A. Schulze, P. Thomas, and S. Schmitt-Rink, Phys. Rev. B **46**, 7252 (1992); K. Leo, P. Haring Bolivar, F. Brüggemann, R. Schwedler, and K. Köhler, Solid State Commun. **84**, 943 (1992); C. Waschke, H. G. Roskos, R. Schwedler, K. Leo, H. Kurz, and K. Köhler, Phys. Rev. Lett. **70**, 3319 (1993).
[5] V. G. Lyssenko, G. Valušis, F. Löser, T. Hasche, K. Leo, M. M. Dignam, and K. Köhler, Phys. Rev. Lett. **79**, 301 (1997).
[6] M. B. Dahan, E. Peik, J. Reichel, Y. Castin, and C. Salomon, Phys. Rev. Lett. **76**, 4508 (1996); S. R. Wilkinson, C. F. Bharucha, K. W. Madison, Q. Niu, and M. G. Raizen, *ibid.* **76**, 4512 (1996).
[7] S. R. Wilkinson, C. F. Bharucha, M. C. Fischer, K. W. Madison, P. R. Morrow, Q. Niu, B. Sundaram, and M. Raizen, Nature (London) **387**, 575 (1997).
[8] H.-B. Braun and D. Loss, J. Appl. Phys. **76**, 6177 (1994); in *Quantum Tunneling of Magnetization—QTM '94*, edited by L. Gunther and B. Barbara (Kluwer, Dordrecht, 1995); D. Loss, in *Dynamical Properties of Unconventional Magnetic Systems*, edited by A. T. Skjeltorp and D. Sherrington (Kluwer, Dordrecht, 1998).
[9] H.-B. Braun and D. Loss, Phys. Rev. B **53**, 3237 (1996).
[10] J. Villain, Physica B **79**, 1 (1975).
[11] H.-B. Braun and D. Loss, Int. J. Mod. Phys. B **10**, 219 (1996).
[12] J. B. Torrance, Jr. and M. Tinkham, Phys. Rev. **187**, 595 (1969); D. F. Nicoli and M. Tinkham, Phys. Rev. B **9**, 3126 (1974).
[13] H.-J. Mikeska, S. Miyashita, and G. H. Ristow, J. Phys.: Condens. Matter **3**, 2985 (1991).
[14] For a review, see for example, H.-J. Mikeska and M. Steiner, Adv. Phys. **40**, 191 (1991).
[15] N. Ishimura and H. Shiba, Prog. Theor. Phys. **63**, 743 (1980).
[16] H. Yoshizawa, K. Hirakawa, S. K. Satija, and G. Shirane, Phys. Rev. B **23**, 2298 (1981).
[17] J. P. Boucher, L. P. Regnault, J. Rossat-Mignod, Y. Henry, J. Bouillot, and W. G. Stirling, Phys. Rev. B **31**, 3015 (1985).
[18] S. E. Nagler, W. J. L. Buyers, R. L. Armstrong, and B. Briat, Phys. Rev. Lett. **49**, 590 (1982).
[19] S. E. Nagler, W. J. L. Buyers, R. L. Armstrong, and B. Briat, Phys. Rev. B **28**, 3873 (1983).
[20] K. Adachi, J. Phys. Soc. Jpn. **50**, 3904 (1981); J. P. Boucher, G. Rius, and Y. Henry, Europhys. Lett. **4**, 1073 (1987); H. Kikuchi and Y. Ajiro, J. Phys. Soc. Jpn. **58**, 2531 (1989).
[21] Y. Ajiro, H. Kikuchi, T. Okita, M. Chiba, K. Adachi, M. Mekata, and T. Goto, J. Phys. Soc. Jpn. **58**, 390 (1989); T. Kohmoto, T. Goto, S. Maegawa, N. Fujiwara, Y. Fukuda, M. Kunitomo, and M. Mekata, Phys. Rev. B **57**, 2936 (1998).
[22] I. Mogi, N. Kojima, Y. Ajiro, H. Kikuchi, T. Ban, and I. Tsujikawa, J. Phys. Soc. Jpn. **56**, 4592 (1987).
[23] E. E. Mendez and G. Bastard, Phys. Today **46** (6), 34 (1993).
[24] *Handbook of Mathematical Functions*, edited by M. Abramowitz and I. A. Stegun (Dover, New York, 1972).
[25] E. E. Mendez, F. Agullo-Rueda, and J. M. Hong, Phys. Rev. Lett. **60**, 2426 (1988).
[26] See for example, Y. Imry, *Introduction to Mesoscopic Physics* (Oxford University Press, Oxford, 1997).
[27] E. N. Economou, *Green's Functions in Quantum Physics* (Springer, Berlin, 1983).
[28] D. Forster, *Hydrodynamic Fluctuations, Broken Symmetry, and Correlation Functions* (Benjamin-Cummings, Reading, MA, 1983).
[29] An oscillation amplitude of less than one lattice constant may present conceptual difficulties in the semiclassical description of a particle following a definite trajectory in space-time. In a fully quantum treatment, such difficulties do not arise because the description is not in terms of definite trajectories, but rather in terms of a quantum expectation value for the soliton's position (which can assume values other than integer multiples of the lattice constant).
[30] L. E. Ballentine, *Quantum Mechanics* (Prentice Hall, Englewood Cliffs, New Jersey, 1990).
[31] K. Takeda, S.-I. Matsukawa, and T. Haseda, J. Phys. Soc. Jpn. **30**, 1330 (1971).
[32] K. Takeda and M. Wada, J. Phys. Soc. Jpn. **50**, 3603 (1981).
[33] R. E. Greeney, C. P. Landee, J. H. Zhang, and W. M. Reiff, Phys. Rev. B **39**, 12 200 (1989).
[34] A. Narath and J. E. Schirber, J. Appl. Phys. **37**, 1124 (1966).
[35] Equation (26) implicitly assumes translational invariance. Although the b field in $H_{1\text{-sol}}$ breaks this symmetry, Eq. (26) is nevertheless correct since the *full* Hamiltonian (2) is translationally invariant.